Proceedings of the 2005 IEEE/ASME
International Conference on Advanced Intelligent Mechatronics
Monterey, California, USA, 24-28 July, 2005

Automated Modelling of Cartridge Valve Flow Mapping

Song Liu and Bin Yao

Abstract— **Proportional poppet-type cartridge valves are the key elements of the energy saving programmable valves, which have been shown in our previous studies to be able to achieve excellent motion control performance while significantly saving energy usage. Unlike costly conventional four-way valves, the cartridge valve has simple structure and is easy to manufacture, but its complicated mathematical model makes the controller design and implementation rather difficult. Our previous works used either an off-line individually calibrated or manufacturer supplied flow mappings as the model of the cartridge valves. Neither method is ideal for industrial wide applications as the former method is time-consuming and needs trained engineers with additional flow sensors while the later leads to significantly degraded control performance due to the inaccuracy of the manufacturer supplied flow mappings. To solve this practically very significant problem, this paper focuses on the automated modelling of the cartridge valve flow mapping without using any extra sensors and removing the valves from the system. The estimation of the flow mapping is based on the pressure dynamics in the hydraulic cylinder with consideration of some unknown parameters like effective bulk modulus of fluid. Experimental results are obtained to illustrate the effectiveness and practicality of the proposed novel automated modelling method.**

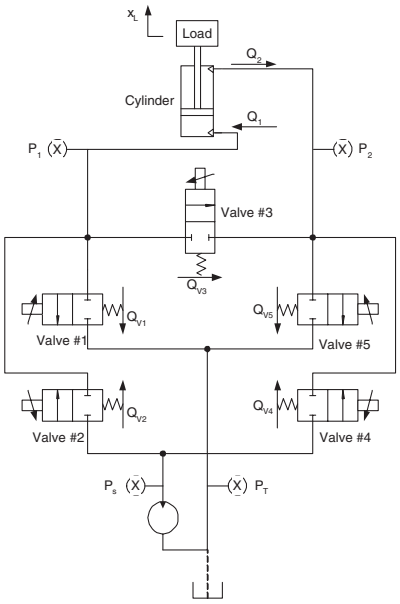

Fig. 1. Energy Saving Programmable Valves.

I. INTRODUCTION

The energy saving programmable valves, a combination of five independently controlled cartridge valves shown in Fig. 1, have been shown in our previous studies [1], [2] to successfully achieve the dual objectives of high level motion control performance and significant energy saving. The great ability of the programmable valves comes from the decoupled meter-in and meter-out flows, the true cross port regeneration flow, and the increased flexibility and controllability of a multiple-input system. The key physical element of the programmable valves is the proportional poppet type cartridge valve, a low accuracy but fast response valve widely used in industry due to its small size and low cost [3], [4].

The much faster response of the poppet type cartridge valves makes it more reasonable to neglect valve dynamics in the overall controller design process [5]; neglecting valve dynamics significantly simplifies the design of advanced nonlinear adaptive robust controllers [6] and has been a common practice in almost all advanced controls of hydraulic systems recently developed. With this simplification, the proportional cartridge valve can be modelled as a static nonlinear flow mapping from the input signal and the pressure drop across the valve into the flow rate through the valve. However, unlike the conventional four-way valves, the mathematical model of the cartridge valve flow mapping is much more complicated and cannot simply be described by some analytical nonlinear equations [7], [8], [9], [10]. Due to this practical problem, though cartridge valves have such desirable physical properties like faster response and the ability of by-passing the sandwiched deadband control problem of conventional four-way valves [5], their use has been traditionally limited to low cost applications where precision motion control is not of major concern. Our previous research works on the control of the programmable valves are based on either the individually calibrated valve flow mappings or the manufacturer supplied flow mapping. Using the individually calibrated flow mappings of the cartridge valves and a properly design adaptive robust controller (ARC), it is shown in [2], [5] that control performance as good as, if not much better than the system using expensive servo valves, can be achieved. However, in addition to the need of a flow calibration system that increases cost, removing the cartridge valves from the system, installing them into the calibration system and individually calibrating each of the five cartridge valves are very time consuming tasks, which would prohibit the widespread use of the programmable valves in industry. On the other hand, though the manufac-

The work is supported in part through the National Science Foundation under the grant CMS-0220179.

S. Liu is a Ph.D Research Assistant at the School of Mechanical Engineering, Purdue University, W. Lafayette, IN 47907, USA liu1@ecn.purdue.edu

B. Yao is an Associate Professor at the School of Mechanical Engineering, Purdue University, W. Lafayette, IN 47907, USA byao@ecn.purdue.edu

turer supplied flow mapping can be used to design stable adaptive robust controllers as done in our previous study [11], the large modelling error of the manufacturer supplied flow mapping significantly limits the achievable control performance in practice. Thus, automated and yet accurate on-board modelling of cartridge valve flow mappings without taking the cartridge valves off the system becomes the key to the widespread use of programmable valves without having a compromised control performance, which is the focus of the paper and serves as a practical example of the integrated mechatronics design philosophy of trading system hardware complexity with advanced modelling and controls.

In order to model the valve flow mappings, one needs to know the input signal to the valve, the pressure drop across the valve and the flow rate going through the valve. The input signal and the pressure drops are usually known or measured. However, there are no sensors to measure the flow rate in an actual system. In [12], an attempt was made to build a flow rate observer based on the pressure dynamics of the controlled system via the sliding mode observer design technique. Because the flow rate appears in the input channel and is not a state in the pressure dynamics, the resulting flow rate observers are subject to certain unavoidable parametric uncertainties such as the effective bulk modulus of fluid due to the changing working conditions. In this paper, a conceptually different approach will be taken. Namely, instead of determining the model parameters of the flow mapping based on the explicit flow rate measurement or estimation, the flow mapping model parameters and other unknown system parameters will be determined simultaneously from the pressure dynamics of the controlled system via certain intelligent integration of on-line parameter estimation algorithms and neural network type nonlinear function modelling techniques. Experimental conditions for accurate parameter estimations are carefully examined to obtain practical on-board tests that can be run for accurate modelling of all valve flow mappings. Comparative experimental results are presented to illustrate the effectiveness and the achievable control performance of the proposed method in implementation.

II. PROBLEM FORMULATION

Neglecting the valve dynamics, all valves can be modelled as a static function mapping the input signal and the pressure drop across the valve into the metered flow rate:

$$Q(u,\Delta P) = C_d A_v\big(x_v(u,\Delta P)\big)\sqrt{\tfrac{2}{\rho}}\sqrt{\Delta P} \qquad (1)$$

where $Q(u,\Delta P)$ is the metered flow rate through the valve orifice, C_d is the discharge coefficient, $A_v(x_v)$ represents the flow area, which is a function of the valve opening x_v, and x_v depends on the input signal u and the pressure drop ΔP across the orifice, ρ is the fluid mass density.

For conventional four-way valves such as the servo valves or the proportional directional control (PDC) valves, A_v is a linear function of x_v, which is only a linear function of input u and not affected by ΔP, therefore the flow mapping model for four-way valves can be simplified to an analytical nonlinear function as:

$$Q = k_q u\sqrt{\Delta P} \qquad (2)$$

where k_q is the lumped valve parameter. As the above flow mapping involves at most one unknown parameter k_q, it is quite easy to obtain a reliable estimate of k_q through either off-line or on-line parameter estimation algorithm.

For the cartridge valves (1), the relationship between A_v and x_v is highly nonlinear and depends on the specific valve construction structure; cartridge valves from different manufactures may have different nonlinear function to connect x_v and A_v. Furthermore, the pressure drop ΔP affects the valve opening as well and cannot be expressed by simple analytical nonlinear functions like (2). In fact, the function $x_v(u,\Delta P)$ is very complicated and highly nonlinear – usually contains some deadband regions and hard limits [13], [2], [5]. One has to treat the cartridge valve flow mapping as an unknown nonlinear function $Q(u,\Delta P)$ and seek other approach to deal with this problem.

One of the powerful tools to approximate or estimate unknown functions is the neural network. The basic idea is to decompose an unknown function into a sum of a large number of neurons with their own weighting factors and use some feedback mechanisms to adjust the weighting factors until the estimation error is minimized [14]. With this tool, the nonlinear flow mapping function can be decomposed as:

$$Q(u,\Delta P) = \bar{Q}(u,\Delta P) + \Delta, \qquad \bar{Q} = \varphi_N^T(u,\Delta P)\cdot w_N \qquad (3)$$

where $\varphi_N^T = [\varphi_1, \varphi_2, ..., \varphi_n]$ is a finite dimension vector of basis functions or neurons, and $w_N^T = [w_{N1}, w_{N2}, ..., w_{Nn}]$ is a vector of unknown parameters or weighting factors, and Δ represents the approximation or modelling error. However, straightforward application of the above neural network approximation seldom leads to satisfactory flow mapping modelling due to the following practical limitation. Namely, to have a reasonably small approximation error Δ, a huge number of neurons (i.e., large n) have to be used. This is especially true for the cartridge valve flow mapping due to the non-smoothness of the cartridge flows caused by the discontinuous frictions of the valve and the difficulty of traditional neural networks in approximating non-smooth functions. Consequently, to obtain the flow mapping model $\bar{Q}(u,\Delta P)$, huge number of parameters w_N have to be adapted or estimated simultaneously from the limited experimental data sets, which makes it impossible to use the well-known parameter estimation algorithms having better converging properties due to the difficulty of running on-board experiments to satisfy the experimental conditions needed by those algorithms. For example, the least square estimation (LSE) algorithm needs the persistent excitation condition for parameter convergence, which, loosely speaking, can be satisfied only if rich enough data sets covering the entire working ranges of the control input u and the pressure drop ΔP are available. However, for on-board flow modelling where the valves cannot be removed from the actual system, ΔP is not an experimental variable that can be freely controlled and there is no way to conduct experiments that cover the

entire range of ΔP. To by-pass this problem, localized basis functions will be used as detailed later.

Since the actual valve flow rates cannot be measured, they have to be estimated based on other available on-board measurements as follows. Neglecting cylinder leakages, the pressure dynamics in the head-end side and the rod-end side of the cylinder can be written as [15]:

$$\begin{aligned} \frac{V_1(x)}{\beta_e}\dot{P}_1 &= -A_1\dot{x} + Q_1(u_1,\Delta P_1) \\ \frac{V_2(x)}{\beta_e}\dot{P}_2 &= +A_2\dot{x} - Q_2(u_2,\Delta P_2) \end{aligned} \tag{4}$$

where $V_1(x)$ and $V_2(x)$ are the total cylinder volumes of the head-end and rod-end sides including connecting hose volumes respectively, x is the displacement of the cylinder rod, β_e is the effective bulk modulus, P_1 and P_2 represent the pressures in the head-end and rod-end sides respectively, A_1 and A_2 are the head-end and rod-end ram areas of the cylinder, Q_1 and Q_2 are the supply and return flow rates respectively, u_1 and u_2 are the input signals to the valves, and ΔP_1 and ΔP_2 are the pressure drops across the valves. In (4), A_1 and A_2 are known parameters, u_1 and u_2 are control signals sent out by the controller, x, P_1, P_2, ΔP_1 and ΔP_2 are measurable, and $V_1(x)$ and $V_2(x)$ are calculable. The effective bulk modulus β_e is usually an unknown parameter and changes significantly with working conditions. Since the pressure dynamics in the rod-end side has the same form as the one in the head-end side, in the following, only the head-end pressure dynamics is used to demonstrate how to solve the problem.

Define $\theta_{\beta_e} = \frac{1}{\beta_e}$, and assume that the nonlinear flow rate $Q_1(u_1,\Delta P_1)$ is decomposed into the form given by (3), the head-end pressure dynamics can then be re-written as:

$$A_1\dot{x} = -V_1(x)\dot{P}_1 \cdot \theta_{\beta_e} + \varphi_N(u_1,\Delta P_1)^T \cdot \theta + \Delta \tag{5}$$

Defining $\varphi_{new}^T = [-V_1(x)\dot{P}_1 \quad \varphi_N(u_1,\Delta P_1)^T]$ and $\theta_{new}^T = [\theta_{\beta_e} \quad \theta^T]$, (5) can be written in a compact form as

$$A_1\dot{x} = \varphi_{new}^T \cdot \theta_{new} + \Delta \tag{6}$$

(6) is in the standard linear regression form with respect to the unknown parameters θ_{new} with $y = A_1\dot{x}$ being the model output and Δ as the model error; both the model output and the regressor can be calculated based on the on-board sensor measurements. Thus, the original problem of automated on-board flow mapping modelling in the presence of unknown system parameters is transformed into the tractable problem of accurate parameter estimation based on the linear regression model (6). The rest of the paper thus focuses on the selection of suitable basis functions $\varphi_N(u_1,\Delta P_1)$, the design of experiments, and the use of the least square algorithm (LSE) to minimize the effect of model error Δ for accurate parameter estimation.

III. LOCALIZED BASIS FUNCTIONS AND SMOOTH BLENDING FOR APPROXIMATION OF TWO-DIMENSIONAL FUNCTIONS

To better explain the underline working principles of the proposed method, for time being, it is assumed in this section that the valve flow rate $Q(u,\Delta P)$ is available for the flow mapping modelling, i.e., assuming that ceratin on-board experiments that cover all possible actual working conditions have been performed with the inputs and the measured valve pressure drops and the valve flow rate given by $\{u(t),\Delta P(t),Q(t),t = 1,2,\ldots,N\}$ respectively, where N represents the total number of sample data from all experiments. In this case, if the neural network type flow mapping model given by (3) is used, then,

$$[Q] = \Phi \cdot \theta + [\Delta] \tag{7}$$

where $[Q] = [Q(1), \ Q(2), \ ..., \ Q(N)]^T$ is the vector of flow rate measurements, $\Phi = [\varphi_N(u(1),\Delta P(1)), \ \varphi_N(u(2),\Delta P(2)), \ ..., \ \varphi_N(u(N),\Delta P(N))]^T$ can be calculated based on the input and the measured valve pressure drops, and $[\Delta] = [\Delta(1), \ \Delta(2), \ ..., \ \Delta(N)]^T$ is the vector of neural network approximation errors which are bounded but unknown. If Φ has full column rank, then the optimal estimation of θ in the sense of the least square estimation (LSE) error is given by

$$\hat{\theta} = \Phi^+ \cdot [Q] \tag{8}$$

where $\Phi^+ = (\Phi^T\Phi)^{-1}\Phi^T$ is the pseudo inverse of Φ. Substituting (7) into (8), the LSE parameter estimation error $\tilde{\theta} = \hat{\theta} - \theta$ is given by

$$\tilde{\theta} = \Phi^+[\Delta] = (\Phi^T\Phi)^{-1}\Phi^T[\Delta] \tag{9}$$

As discussed in section II, with the above traditional neural network model, to have a reasonable small model approximation error $[\Delta]$, the dimension of the basis functions n has to be very high, especially when the unknown function to be approximated has discontinuity or non-differentiable points. This fact plus the additional practical limitation of not being able to run on-board experiments to excite the system for variety of pressure drops makes it impossible to satisfy the condition needed to apply the above LSE algorithm – Φ being full column rank, or equivalently, $\Phi^T\Phi$ being invertible. To solve this problem, in the following, localized basis functions with smooth blending will be used.

Due to the fact that the cartridge valve can only accept bounded input signal u ranging from 0 volt to 10 volt and the pressure drop is also limited by the supply pressure which is about 6900KPa (1000PSI), the flow mapping is defined only on a compact support. It is reasonable to cut the support on $u-\Delta P$ surface into small blocks, where u_{Nx} and P_{Ny} represent the maximal values of u and ΔP respectively. Each block is named after the indices of u and P, e.g. I_{ij}, as shown in Fig. 2. The distances between u_i and u_{i+1} or P_i and P_{j+1} do not have to be equally spaced. As the function approximation will be done on each small block instead of on the entire region, *a priori* knowledge about the flow mapping can be used to help choose the spacing to have a reasonable good model approximation accuracy while minimizing the number of blocks needed. For example, it is known that the deadband may happen around some input values though the exact value is not known. Thus, relatively small spacing should be used

in regions near those input values. On the other hand, at the regions where one knows the flow mapping may not change drastically, relatively larger spacings can be used to reduce the computation load.

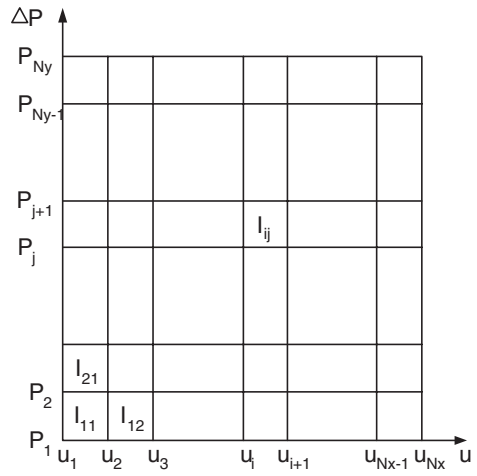

Fig. 2. Cutting the $u-\Delta P$ surface into small blocks.

On each small block I_{ij}, the valve flow rate does not change drastically and may be expressed as a Taylor series with respect to the nominal point :

$$Q(u,\Delta P)|_{(u,\Delta P)\in I_{ij}} = Q(\bar{u}_i,\Delta\bar{P}_j) + \frac{\partial Q}{\partial u}|_{(\bar{u}_i,\Delta\bar{P}_j)}\tilde{u} + \frac{\partial Q}{\partial \Delta P}|_{(\bar{u}_i,\Delta\bar{P}_j)}\tilde{P} + \frac{1}{2}\frac{\partial^2 Q}{\partial u^2}|_{(\bar{u}_i,\Delta\bar{P}_j)}\tilde{u}^2 + \frac{1}{2}\frac{\partial^2 Q}{\partial \Delta P^2}|_{(\bar{u}_i,\Delta\bar{P}_j)}\tilde{P}^2 + \frac{1}{2}\frac{\partial^2 Q}{\partial u\partial \Delta P}|_{(\bar{u}_i,\Delta\bar{P}_j)}\tilde{u}\tilde{P} + \Delta \quad (10)$$

where $(\bar{u}_i,\Delta\bar{P}_j)$ represents the nominal working point in the block of I_{ij}, $\tilde{u} = u-\bar{u}_i$ and $\tilde{P} = \Delta P - \Delta\bar{P}_j$, and Δ represents all higher order terms. *A priori* knowledge about the flow mapping as well as the required model approximation accuracy can be used to determine how many terms to keep. For simplicity, in this paper, all terms up to second order are kept while all higher order terms are considered as modelling error. The valve flow rate in the block of I_{ij} is therefore approximated by a model given by

$$\bar{Q}(u,\Delta P)|_{(u,\Delta P)\in I_{ij}} = \varphi_{ij}^T\cdot\theta_{ij} \quad (11)$$

where $\varphi_{ij}^T = \begin{cases}[1,\ \tilde{u},\ \tilde{P},\ \tilde{u}^2,\ \tilde{P}^2,\ \tilde{u}\tilde{P}] & (u,\Delta P)\in I_{ij},\\ [0,\ 0,\ 0,\ 0,\ 0,\ 0] & \text{otherwise.}\end{cases}$ and $\theta_{ij} = [Q(\bar{u}_i,\Delta\bar{P}_j),\ \frac{\partial Q}{\partial u}|_{(\bar{u}_i,\Delta\bar{P}_j)},\ \frac{\partial Q}{\partial \Delta P}|_{(\bar{u}_i,\Delta\bar{P}_j)},\ \frac{\partial^2 Q}{\partial u^2}|_{(\bar{u}_i,\Delta\bar{P}_j)},\ \frac{\partial^2 Q}{\partial \Delta P^2}|_{(\bar{u}_i,\Delta\bar{P}_j)},\ \frac{\partial^2 Q}{\partial u\partial \Delta P}|_{(\bar{u}_i,\Delta\bar{P}_j)}]^T \in \mathbb{R}^6$.

With the above local approximations, on the entire region, the approximated flow mapping model is:

$$\bar{Q}(u,\Delta P) = \sum_{j=1}^{N_y}\sum_{i=1}^{N_x}\varphi_{ij}^T\cdot\theta_{ij} \quad (12)$$

which is in the form of (3) with $\varphi_N^T = [\varphi_{11}^T,\ \varphi_{12}^T,\ldots,\ \varphi_{1N_y}^T,\ \varphi_{21}^T,\ \ldots,\ \varphi_{ij}^T,\ \ldots,\ \varphi_{N_xN_y}^T]$, $\theta^T = [\theta_{11}^T,\ \theta_{12}^T,\ldots,\ \theta_{1N_y}^T,\ \theta_{21}^T,\ \ldots,\ \theta_{ij}^T,\ \ldots,\ \theta_{N_xN_y}^T]$. However, different from (3), the basis functions φ_{ij} in (12) are localized, which enables the accurate parameter estimations to be carried out for individual blocks where sufficient data exist and the condition for applying the LSE algorithm is satisfied. Those regions normally correspond to the actual working ranges that the system is likely to operate, and thus precise flow modelling in those regions are important for good control performance as well. The details are given below.

Regroup the sample data according to the blocks they belong to. For simplicity, assume that $\{u(t),\Delta P(t),Q(t),t=1,2,\ldots,N_{ij}\}$ are the set of sample data falling into the block I_{ij}, i.e., $(u(t),\Delta P(t))\in I_{ij},\ \forall t=1,2,\ldots,N_{ij}$ where N_{ij} represents the number of points. From (10) and (11), a similar form as (7) can be obtained for the block I_{ij}:

$$[Q(u,\Delta P)]|_{(u,\Delta P)\in I_{ij}} = \Phi_{ij}\cdot\theta_{ij} + [\Delta] \quad (13)$$

where $[Q(u,\Delta P)]|_{(u,\Delta P)\in I_{ij}}$ represents the vector of the measured valve flow rate and $\Phi_{ij} = [\varphi_{ij}(1),\ \varphi_{ij}(2),\ \ldots,\ \varphi_{ij}(N_{ij})]^T$. If $\Phi_{ij}^T\Phi_{ij}$ is invertible – a condition that can be satisfied relatively easily due to the small number of parameters to be estimated, then, the experimental data are rich enough to give a good LSE estimate of θ_{ij} on the block I_{ij}:

$$\hat{\theta}_{ij} = (\Phi_{ij}^T\Phi_{ij})^{-1}\Phi_{ij}^T\cdot[Q(u,\Delta P)]|_{(u,\Delta P)\in I_{ij}} \quad (14)$$

In practice, one can check the condition number of $\Phi_{ij}^T\Phi_{ij}$ instead of its invertibility to make sure the above estimation is numerically well-conditioned for reliable estimations.

For the blocks where $\Phi_{ij}^T\Phi_{ij}$ is not invertible or ill-conditioned, it is impossible to have an accurate estimate of θ_{ij} as the experimental data obtained do not provide enough information on I_{ij} for flow modelling. Therefore one should not force the system to estimate θ_{ij}. The flow mapping in these regions should be obtained via other means such as the extrapolation based on the flow models obtained for the blocks where rich data are available.

The above method is to pass the signal through a discontinuous rectangular window defined on each block I_{ij}, which would usually results in discontinuous estimation of which discontinuity happens at the block boundaries. To avoid these discontinuity artifacts, it is necessary to use smooth windows [16]. The lapped projectors, which split signal in orthogonal components with overlapping supports [16], will be used to smooth the discontinuous estimation.

For simplicity, two orthogonal projectors that decompose any $f\in L^2(\mathbb{R})$ in two orthogonal components P^+f and P^-f whose supports are $[-1,\ +\infty)$ and $(-\infty,\ 1]$ respectively are constructed for demonstration.

$$\begin{aligned} P^+f(t) &= \beta(t)[\beta(t)f(t)+\beta(-t)f(-t)]\\ P^-f(t) &= \beta(-t)[\beta(-t)f(t)-\beta(t)f(-t)]\end{aligned} \quad (15)$$

where β is a monotone increasing profile function, such as $\beta(t) = \begin{cases}0 & \text{if } t<-1\\ 1 & \text{if } t>1\end{cases}$ and $\beta^2(t)+\beta^2(-t)=1 \quad \forall t\in[-1,1]$

Theorem 1: (Coifman and Meyer) The operators P^+ and P^- are orthogonal projectors respectively on W^+ and W^-. The spaces W^+ and W^- are orthogonal and $P^++P^- = Identity$.

The proof of the theorem can be seen in [16]. The projectors can be easily shifted to $[a-\eta,\ +\infty)$ and $(-\infty,\ a+\eta]$ or repeated at different locations to perform a signal decomposition into orthogonal pieces whose supports overlap. It is also straight forward to extend the projectors from one-dimensional to two-dimensional. There exist several well know lapped orthogonal bases, such as the family of local cosine functions [16].

IV. AUTOMATED ON-BOARD MODELLING OF THE VALVE FLOW MAPPINGS

As discussed in section II, the actual valve flow rate is not measured in on-board experiments. However, with φ_{new} and θ_{new} in (6) defined as $\varphi_{new}^T = [-V_1(x)\dot{P}_1,\ \varphi_{11}^T,\ \varphi_{12}^T, \dots,\ \varphi_{1N_y}^T,\ \varphi_{21}^T,\ \dots,\ \varphi_{ij}^T,\ \dots,\ \varphi_{N_xN_y}^T]$ and $\theta_{new}^T = [\theta_{\beta_e},\ \theta_{11}^T,\ \theta_{12}^T, \dots,\ \theta_{1N_y}^T,\ \theta_{21}^T,\ \dots,\ \theta_{ij}^T,\ \dots,\ \theta_{N_xN_y}^T]$, the same estimation technique as in Section III can be used to obtain the estimates of θ_{β_e} and θ_{ij} simultaneously for the blocks where the local persistent excitation condition is satisfied.

In practice, although x, $\dot{x}$, ΔP_1 and $V_1(x)$ are measurable or calculable, $\dot{P}_1$ is neither measurable nor calculable from differentiating P_1 without a low pass filter due to the very noisy pressure measurement. In order to make (6) implementable for parameter estimation algorithms, a low pass filter, such as the one in (16), can be applied to the regressor φ_{new} as well as the virtual output $A_1\dot{x}$.

$$H_f(s) = \frac{\omega_n^2}{s^2+2\zeta\omega_n s+\omega_n^2} \tag{16}$$

where ζ and ω_n are the damping ratio and natural frequency of the low pass filter respectively. Applying the linear filter (16) to both sides of Eq. (6) leads to:

$$A_1\dot{x}_f = \varphi_{newf}^T \cdot \theta_{new} + \Delta_f \tag{17}$$

where $\dot{x}_f$, φ_{newf}^T and Δ_f represent the filtered $\dot{x}$, φ_{new} and Δ. With (17), the effect of measurement noise is reduced and the same estimation technique as in Section III can still be used to obtain the estimates of θ_{β_e} and θ_{ij} simultaneously for the blocks where the local persistent excitation condition is satisfied.

V. SIMULATIONS AND EXPERIMENTS

Simulations and experiments are done to illustrate the proposed automated flow mapping modelling method. In the experiments, the programmable valves are used to control the boom motion of the three degree-of-freedom hydraulic robot arm at the Ray. W. Herrick Laboratories. The working mode selection and the coordinate controller design for the programmable valves can be found in [2]. For simplicity, the following study is concentrated on the automated modelling of the flow mapping for the valve #2 shown in Fig. 1 for the programmable valves. The boom motion is controlled to track a swiped sinusoidal reference trajectory, whose frequency varies from 0.1 Hz to 0.5 Hz over 80 seconds. Fig. 3 shows how the blocks are generated and where the obtained experimental data locate. The fine grids between 1 volt and 4 volts for the control input is for more accurate flow estimation to deal with the unknown deadband in this region.

TABLE I
ESTIMATED FLOW MAPPING VS. TRUE VALUE

	4v	5v	6v	7v
4.5MPa	7.33 8.00	12.02 11.83	17.79 17.57	22.96 22.60
5MPa	8.20 8.00	12.44 12.22	17.37 17.18	22.62 21.95
5.5MPa	7.98 7.97	12.02 12.00	*NA* 16.39	*NA* 20.61

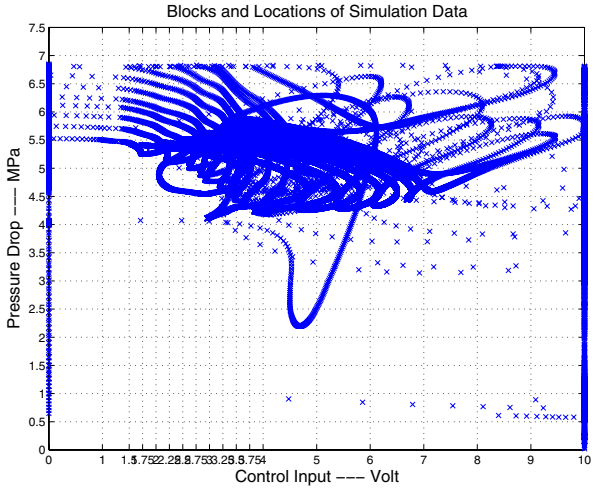

Fig. 3. Blocking and Location of Experimental Data.

It is obvious that the obtained on-board experiment data do not cover the entire region, and it is impossible to have flow estimates in the blocks which suffer low data or no data at all. However, with the localized orthogonal basis functions and by checking the condition number of $\Phi_{ij}^T\Phi_{ij}$ on each block, one can easily control the estimation process with the proposed method. For example, by setting the threshold for the condition number as 1×10^8 and only estimating the flow mappings for blocks having the condition number less than the threshold, the estimated flow mapping with extrapolations is compared with the individually calibrated one as shown in Table I. In I, the flow rate has a unit of L/min, the upper number represents the value given by the estimated flow mapping with the proposed method and the lower number the value from individually calibrated one. It is seen that both values are quite close to each other, illustrating the reasonable modelling accuracy of the proposed method.

In the above study, neither the valve control input u nor the pressure drop ΔP is arbitrarily controlled. This results in lack of data in a lot of regions. For more accurate flow mapping estimation, one can simplify the two-dimensional flow mapping into a series of one-dimensional mappings, i.e., fix the control input u and estimate a bunch of one-

dimensional function described as follows:

$$Q(u,\Delta P)|_{u=u_i} = Q_i(\Delta P), \quad i = 1,2,...,Nx \tag{18}$$

Figure 4 shows one of the experimentally estimated flow mappings with this method.

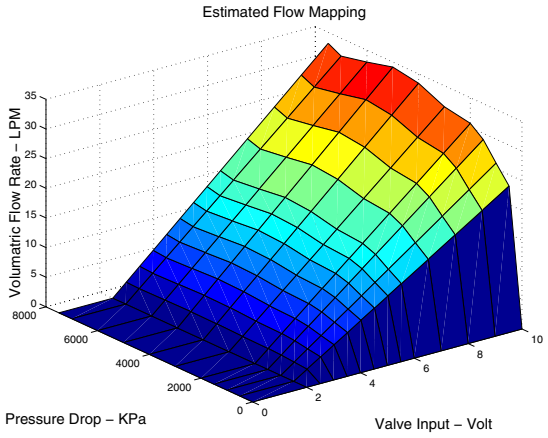

Fig. 4. Estimated Cartridge Valve Flow Mapping.

To illustrate the effectiveness of the proposed method, the above estimated flow mappings along with the individually calibrated one in [2], [5] or the manufacture supplied one in [11] are used in the same ARC controller to control the boom motion of the hydraulic arm respectively. Specifically, the ARC controller design by Liu and Yao in [11] with the control gains set to 16 and adaptation turned off is used for all the experiments. The tracking performance for the typical point-to-point industrial motion trajectory shown in Fig. 5 are shown in the second plot of Fig. 5. Although the controller with the experimentally estimated flow mappings performs not as good as the one with individually calibrated flow mappings due to the limited on-board experimental data used in the flow mapping estimation, it does perform better than the one using the manufacturer supplied flow mappings.

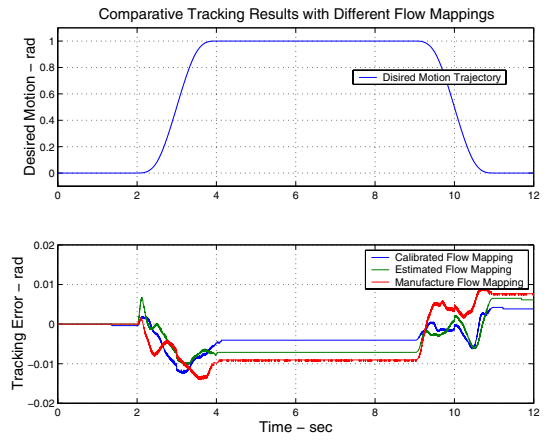

Fig. 5. Comparative Tracking Results with Different Flow Mappings.

VI. CONCLUSIONS

Automated on-board modelling of the proportional cartridge valve flow mapping is very important for industrial wide use of the valve in precision motion control applications. Due to the extremely complicated and uncertain model structure of the cartridge valves, it is impossible to formulate the modelling of their flow mappings into some simple parameter estimation problems, not to mention the unavailability of the flow rate measurement and the uncertain parameters in the system dynamics. This paper proposes an approach to decompose and approximate the unknown flow mapping with some localized orthogonal basis functions. The weighting parameters of the basis functions as well as the unknown system parameters are then estimated simultaneously based on the pressure dynamics of the cylinder for regions where sufficient on-board measurement data are available. Preliminary experimental studies have been obtained to demonstrate the feasibility of the proposed method for the automated on-board modelling of the cartridge valve flow mappings and the improvement of control performance with the estimated flow mappings. The method is quite general and can be used in other system identifications.

REFERENCES

[1] S. Liu and B. Yao, "Energy-saving control of single-rod hydraulic cylinders with programmable valves and improved working mode selection," *SAE Transactions - Journal of Commercial Vehicle*, pp. 51–61, 2002, SAE 2002-01-1343, This paper was first presented at IFPE 2002.

[2] ——, "Coordinate control of energy-saving programmable valves," in *ASME International Mechanical Engineering Congress and Exposition*, Wahsington, D.C., 2003, IMECE 2003-42668.

[3] J. J. Pippenger, *Hydraulic Cartridge Valve Technology*. Amalgan Publishing Company, 1990.

[4] T. J. Ulery, "Propotional cartridge valves - economical alternative to large valves," *Agricultural Engineering*, vol. 71, no. 4, p. 11, 1990.

[5] S. Liu and B. Yao, "Programmable valves: a solution to bypass deadband problem of electro-hydraulic systems," in *Proc. of American Control Conference*, Boston, MA., 2004, pp. 4438–4443.

[6] B. Yao, F. Bu, J. T. Reedy, and G. T. Chiu, "Adaptive robust control of single-rod hydraulic actuators: Theory and experiments," *The IEEE/ASME Trans. on Mechatronics*, vol. 5, no. 1, pp. 79–91, 2000.

[7] N. Vaughan and J. Gamble, "The modeling and simulation of a proportional solenoid valve," *Journal of Dynamic Systems, Measurement, and Control*, vol. 118, pp. 120–125, 1996.

[8] N. Vaughan, D. Johnston, and K. Edge, "Numerical simulation of fluid flow in poppet valves," *Journal of Mechanical Engineering Science, Part C, IMech*, vol. 206, pp. 119–127, 1992.

[9] D. Johnston, K. Edge, and N. Vaughan, "Experimental investigation of flow and force characteristics of hydraulic poppet and disc valves," *Journal of Mechanical Engineering Science, Part C, IMech*, vol. 205, pp. 161–171, 1991.

[10] S. Liu, G. Krutz, and B. Yao, "Easy5 model of two position solenoid operated cartridge valves," in *ASME International Mechanical Engineering Congree and Exposition*, New Orleans, Louisiana, 2002, IMECE 2002-39335.

[11] S. Liu and B. Yao, "Adaptive robust control of programmable valves with manufacture supplied flow mapping only," in *IEEE Conference on Decision and Control*, Atlantis, Paradise Island, Bahamas, 2004.

[12] ——, "Sliding mode flow rate observer design," in *Proc. of The 6th International Conference on Fluid Power Transmission and Control*, Hangzhou, P.R. China, 2005.

[13] E. C. Fitch and I. T. Hong, *Hydraulic component design and selection*. BarDyne, Inc, 2001.

[14] S. Haykin, *Neural Networks, A Comprehensive Foundation*, 2nd ed. Pearson Education, 1999.

[15] H. E. Merritt, *Hydraulic Control Systems*. John Wiley & Sons, 1967.

[16] S. mallat, *A Wavelet Tour of Signal Processing*. Academic Press, 1999.